JOURNAL OF Materials CHEMISTRY

Structure and electrical and magnetic properties of $(PTMA)_x[M(Pc)(CN)_2]\cdot y$(solvent) (PTMA = phenyltrimethylammonium and $[M(Pc)(CN)_2]$ = dicyano(phthalocyaninato)M^{III} with M = Co and Fe). Partial oxidation by partial solvent occupation of the cationic site

Masaki Matsuda,[a] Toshio Naito,[a] Tamotsu Inabe,*[a] Noriaki Hanasaki[b] and Hiroyuki Tajima[b]

[a]*Division of Chemistry, Graduate School of Science, Hokkaido University, Sapporo 060-0810, Japan. E-mail: inabe@sci.hokudai.ac.jp*
[b]*Institute for Solid State Physics, The University of Tokyo, Kashiwanoha, Kashiwa, Chiba 277-8581, Japan*

Received 17th January 2001, Accepted 26th June 2001
First published as an Advance Article on the web 21st August 2001

Electrochemical oxidation of PTMA[M^{III}(Pc)$(CN)_2$] (PTMA = phenyltrimethylammonium, Pc = phthalocyaninato, and M = Co or Fe) gives partially oxidized salts $(PTMA)_x[M^{III}(Pc)(CN)_2]\cdot y$(solvent) (solvent = acetonitrile or acetone). The obtained crystals in which the solvent molecules partially occupy the cationic sites are isomorphous regardless of M and solvent. They are highly conducting and metallic behavior is observed in the conductivity and thermoelectric power measurements. In contrast to the Pauli-like behavior of the Co^{III} salt, Curie-like behavior with an anomaly due to antiferromagnetic interactions was observed for the Fe^{III} salt in magnetic susceptibility measurements. The existence of local magnetic moments in the Fe^{III} salt leads to a significant influence on the transport properties, suggesting the existence of π–d interactions in this system.

Metal phthalocyanines, M(Pc)s, are known to form one-dimensional face-to-face stacking conductors, $[M(Pc)]_yX$ (M = Ni, Cu, H_2, Pt, *etc.*; X = I_3, ClO_4, AsF_6, SbF_6, *etc.*).[1–4] Recently, we have reported another type of molecular conductor based on the axially substituted phthalocyanine anions, $[M^{III}(Pc)(CN)_2]^-$ with M = Co and Fe.[5–12] When the anion is electrochemically oxidized, neutral radical crystals[6,7] or partially oxidized salt crystals[8–10] can be obtained. The π–π overlap between the Pc rings is only partial compared with the face-to-face stacking due to the existence of the axial CN ligands, yet the Pc units form effective conduction paths through the π–π overlaps. The most interesting point of this type of conductor is that the dimensionality of the electronic system resulting from the π–π stacking network is varied by the second component of the lattice; *i.e.*, crystal solvents in the neutral radical crystals and cations in the partially oxidized salt crystals.

One merit of utilizing $[M^{III}(Pc)(CN)_2]^-$ as a component of molecular conductors is that one can utilize various cations in the quest for novel partially oxidized salt conductors. We have found that the electrochemical oxidation of the PTMA salts in acetonitrile gives novel conductors. Strangely, in these crystals, both centers of the Pc and cation units were found at 2/*m* symmetry sites in the space group *Pnnm*, so that the stoichiometry is 1 : 1. However, they are highly conducting and have been found to be partially oxidized salts in which the cationic sites are partially occupied by the solvent molecules. In this paper, we describe the preparation, structure, and electrical and magnetic properties of $(PTMA)_x[M^{III}(Pc)(CN)_2]\cdot y$-(solvent) with M = Co and Fe. When the metal is cobalt(III), the octahedral ligand field imposes the low-spin d^6 configuration which is non-magnetic. On the other hand, for iron(III) it imposes the low-spin d^5 configuration with an $S = 1/2$ magnetic moment. This difference has been found to greatly influence the transport properties of the TPP$[M^{III}(Pc)(CN)_2]_2$ (TPP = tetraphenylphosphonium) conductors[8,10] due to the π–d interaction, as represented by the giant negative magnetoresistance.[11] In the present compounds, it has also been found that the existence of a magnetic moment induces a large influence on the physical properties.

Experimental

Materials

The starting simple salt of PTMA$[Co^{III}(Pc)(CN)_2]$ was prepared by the metathesis of $K[Co^{III}(Pc)(CN)_2]$[13] with PTMA·Br in acetonitrile. Since the preparation of the corresponding Fe^{III} salt following a method used for TPP$[Fe^{III}(Pc)(CN)_2]$[10] gave a poor yield, $(PTMA)_2[Fe^{II}(Pc)(CN)_2]$, which was obtained by the metathesis of $K_2[Fe^{II}(Pc)(CN)_2]$[10] with PTMA·Br, was used as the starting salt for the electrolysis.

An electrocrystallization cell equipped with a glass frit between the two compartments was filled with *ca.* 35 ml of an acetonitrile or acetone solution of PTMA$[Co^{III}(Pc)(CN)_2]$ or $(PTMA)_2[Fe^{II}(Pc)(CN)_2]$ (*ca.* 0.7 mmol dm^{-3}). A constant current of typically 1 μA was applied between two platinum electrodes immersed in the solution of each compartment {1–2 weeks for $(PTMA)_x[Co^{III}(Pc)(CN)_2]\cdot y$(solvent) or 1–2 months for $(PTMA)_x[Fe^{III}(Pc)(CN)_2]\cdot y$(solvent)} at 20 °C. The needle crystals grew on the anode surface during the current flow, and were collected by filtration. Other solvent systems adopted were ethanol, *tert*-butylbenzene–acetonitrile or *tert*-butylbenzene–acetone, monohalogen-substituted-benzene–acetonitrile or monohalogen-substituted-benzene–isobutyronitrile, *N,N*-dimethylaniline–propionitrile. None of these, however, gave crystals.

DOI: 10.1039/b100623l

Table 1 Crystal data for $(PTMA)_x[M(Pc)(CN)_2]\cdot y(solvent)$ ($x=0.5$ and $y=1.0$)

	$(PTMA)_x[Fe(Pc)(CN)_2]\cdot y(MeCN)$	$(PTMA)_x[Co(Pc)(CN)_2]\cdot y(MeCN)$	$(PTMA)_x[Fe(Pc)(CN)_2]\cdot y(MeCN)$	$(PTMA)_x[Co(Pc)(CN)_2]\cdot y(Me_2CO)$
Chemical formula	$C_{40.5}H_{26}N_{11.5}Fe$	$C_{40.5}H_{26}N_{11.5}Co$	$C_{40.5}H_{26}N_{11.5}Fe$	$C_{41.5}H_{29}N_{10.5}OCo$
Molecular weight	729.57	732.66	729.57	749.72
Crystal system	Orthorhombic	Orthorhombic	Orthorhombic	Orthorhombic
Space group	*Pnnm*	*Pnnm*	*Pnnm*	*Pnnm*
a/Å	13.900(1)	13.871(1)	13.850(1)	13.668(1)
b/Å	7.332(1)	7.350(1)	7.249(1)	7.310(1)
c/Å	16.317(1)	16.296(1)	16.155(1)	16.371(1)
V/Å^3	1662.9(1)	1661.3(1)	1622.1(2)	1635.7(1)
Z	2	2	2	2
μ(Mo-Kα)/cm^{-1}	5.00	5.68	5.17	5.80
Temperature of data collection/K	295	295	123	113
No. of unique reflections	1979	1978	1930	1950
No. of independent reflections observed	1218 [$I>3\sigma(I)$]	918 [$I>3\sigma(I)$]	1326 [$I>3\sigma(I)$]	1060 [$I>3\sigma(I)$]
R_{int}	0.01	0.06	0.04	0.06
R	0.051	0.047	0.051	0.043
R_w	0.058	0.046	0.053	0.053

X-Ray structure analyses

A Rigaku R-AXIS Rapid imaging plate diffractometer with graphite-monochromated Mo-Kα radiation was used for data collection, and the crystal data are summarized in Table 1.

The structures were solved by a direct method (SIR-92[14]) and all the crystals analyzed were found to be isomorphous. Low-temperature measurements were performed for the confirmation of the electron density distribution at the disordered cation site. Owing to this disorder, including partial replacement by the solvent molecules, the refinement could not be performed with idealized procedures. First, the hydrogen atoms were placed at calculated ideal positions only for the Pc unit. Second, the anisotropic thermal parameters were not applied for the atoms at the cation site, since the electron density is too low due to the disorder. Third, the values of x and y were assigned to 0.5 and 1, respectively, for all the crystals by referring to the results of the thermoelectric power measurements. For the MeCN-inclusive crystals, an additional electron density peak near the phenyl ring of PTMA was found by difference Fourier synthesis. Though the peak corresponds to either end of MeCN, full assignment was not possible due to the positional and orientational disorder of MeCN. Owing to the close proximity of this peak to a carbon atom of the phenyl group, the coordinates of these atoms could not be refined and were fixed at the electron density peak positions. For the Me_2CO-inclusive crystal, an additional electron density peak was also found by the difference synthesis. The degree of disorder in this crystal is much less, and it was possible to assign this peak to the oxygen of Me_2CO from the bond length. When one atomic site is occupied by two types of atoms (N and C), only one was adopted. A full-matrix least-squares technique was employed for the structure refinement using the teXsan program package.[15]

CCDC reference numbers 157358, 157359, 164082 and 164083.

See http://www.rsc.org/suppdata/jm/b1/b100623l/ for crystallographic data in CIF or other electronic format.

Measurements

Electrical conductivities were measured in the temperature range 5–300 K for $(PTMA)_x[Co^{III}(Pc)(CN)_2]\cdot y(solvent)$ or 18–300 K for $(PTMA)_x[Fe^{III}(Pc)(CN)_2]\cdot y(MeCN)$ *in vacuo*. When the sample resistance is low, the normal four-probe method with contacts by gold paste was applied. When the sample resistance exceeds the measurable limit of our four-probe method, the measurement was switched to a two-probe method. The two-probe measurement was also extended to a higher temperature region where the four-probe method gave reliable values, in order to make sure that the contact resistance was small enough and that its temperature dependence was negligible compared with that of the sample crystal. The four- to two-probe switching temperature was 15–25 K for the Co salts and 33–50 K for the Fe salts. The reproducibility was also checked using several crystals. Thermoelectric power measurements were carried out using a system similar to that reported by Chaikin and Kwak[16] under 20 Torr of He gas.

Magnetic susceptibility measurements for randomly oriented sample crystals were performed using a Quantum Design MPMS-5 SQUID susceptometer. The sample container was evacuated and then filled with the He gas. The applied field was 1 T, and the background contribution was separately measured. The diamagnetic core contributions of PTMA and solvents were estimated by the Pascal's constants, and that of the $[M^{III}(Pc)(CN)_2]$ unit was estimated as previously described.[10]

Results and discussion

Crystal growth

The electrocrystallization was strongly dependent on the solvent system used for the electrolysis. Only acetonitrile or acetone gave needle-like crystals on the anode surface. In other cases, precipitation of the oxidized products was scarcely observed. As found in the structure analyses (*vide infra*), some specific solvents partially occupy the cationic sites. Since the cationic sites cannot be replaced by molecules which have simply a similar size and shape as PTMA, such as *tert*-butylbenzene, some electronic properties, *e.g.*, the dipole moment and polarizability, may be more important for the partial occupation of the cationic site. The solvents appear to be completely encapsulated in the lattice, since the crystals are fairly stable even *in vacuo* for the physical measurements.

Molecular and crystal structure of $(PTMA)_x[M^{III}(Pc)(CN)_2]\cdot y(solvent)$

The molecular and crystal structure of $(PTMA)_x[Fe^{III}(Pc)(CN)_2]\cdot y(MeCN)$ at 123 K is shown in Fig. 1. The temperature dependence of the crystal structure is practically negligible, and is isomorphous with $(PTMA)_x[Co^{III}(Pc)(CN)_2]\cdot y(MeCN)$ and $(PTMA)_x[Co^{III}(Pc)(CN)_2]\cdot y(Me_2CO)$. Differences in the molecular structure of the $M(Pc)(CN)_2$ unit are scarcely seen upon replacement of Co^{III} by Fe^{III}, except for slightly longer M–CN bond lengths in the Fe^{III} compound than in the Co^{III} compound due to the larger ionic radius of Fe^{III}. The central metal ion is located at the 2/*m* sites, and one-quarter of the unit is crystallographically independent. Judging from the thermal parameters, there is no structural disorder in the $M(Pc)(CN)_2$ unit.

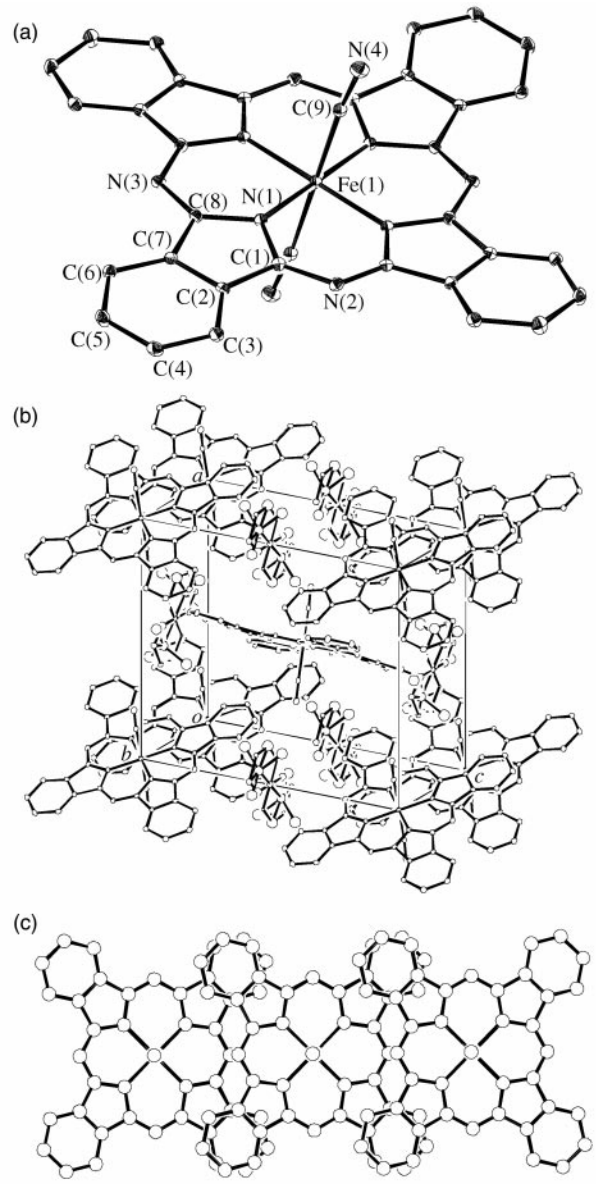

Fig. 1 (a) ORTEP drawing of the $Fe^{III}(Pc)(CN)_2$ unit in $(PTMA)_x[Fe^{III}(Pc)(CN)_2]\cdot y(MeCN)$ at 123 K showing the atom numbering scheme, (b) the crystal structure and (c) the molecular stacking in the $Fe(Pc)(CN)_2$ chain (neighboring molecules are related by a unit translation along the *b*-axis).

On the other hand, the cationic site is rather complicated. The cation sites in $(PTMA)_x[Fe^{III}(Pc)(CN)_2]\cdot y(MeCN)$ and in $(PTMA)_x[Co^{III}(Pc)(CN)_2]\cdot y(Me_2CO)$ are shown in Fig. 2. Since the centers of their sites are also coincident with the 2/*m* symmetry, two opposite orientations of PTMA are superimposed (the phenyl ring of PTMA lies on the mirror plane). If $x=1$ and $y=0$, the structure corresponds to that of the simple salt. However, the crystal structure of $PTMA[Fe^{III}(Pc)(CN)_2]$ has been found to be completely different.[17] At first, the analysis of $(PTMA)_x[Fe^{III}(Pc)(CN)_2]\cdot y(MeCN)$ was performed with $x=1$ and $y=0$, and the resultant PTMA was found to suffer serious deformation and uneven thermal parameters. This suggests the partial replacement of the cationic site by MeCN. The final refinement was then performed with $x=0.5$ and $y=1$. The x value is estimated from the results of the thermoelectric power measurements (*vide infra*), and the remaining vacant sites are assumed to be fully occupied by MeCN or Me_2CO, *i.e.*, $y=1$. For the MeCN-inclusive crystals, an additional peak was found by the difference synthesis [assigned as C(17) in Fig. 2(a)], which corresponds to either end of MeCN. For the Me_2CO-inclusive crystal, an additional peak

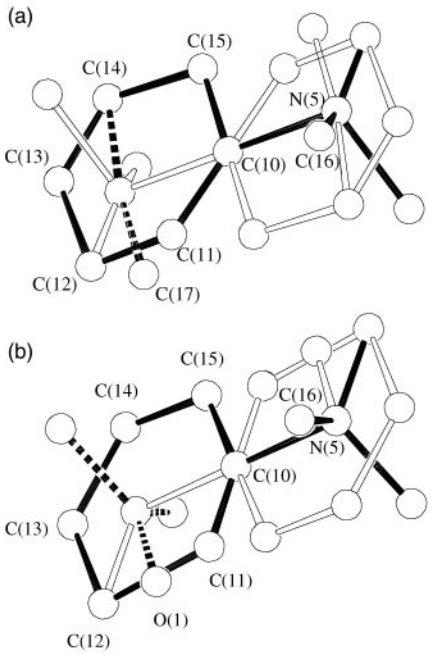

Fig. 2 (a) Atom distributions at the PTMA site in $(PTMA)_x[Fe^{III}(Pc)(CN)_2]\cdot y(MeCN)$ at 123 K ($x=0.5$ and $y=1$) and (b) in $(PTMA)_x[Co^{III}(Pc)(CN)_2]\cdot y(Me_2CO)$ at 113 K ($x=0.5$ and $y=1$). The solid bonds represent the PTMA fragment and the dashed bonds represent (a) the MeCN and (b) Me_2CO fragments.

that corresponds to the oxygen of Me_2CO [assigned as O(1) in Fig. 2(b)] was found. Since the final thermal parameters are fairly normal, the assignment of $y=1$ is close to the actual value.

The $M(Pc)(CN)_2$ units are aligned along the *b*-axis with π–π overlaps between the Pc rings, forming a one-dimensional chain. Each chain is isolated by the arrays of the cationic components. The structure of the one-dimensional chain is shown in Fig. 1(b). The Pc rings are stacked with overlaps at two of the four peripheral benzene rings with an interplanar distance of 3.46 Å for both $(PTMA)_x[Co^{III}(Pc)(CN)_2]\cdot y(MeCN)$ and $(PTMA)_x[Fe^{III}(Pc)(CN)_2]\cdot y(MeCN)$ at 295 K. The effectiveness of this stacking mode has been evaluated from an extended Hückel calculation based on the structural data. The overlap integral between the Pc rings in a chain is calculated to be 9.4×10^{-3} for the Co^{III} salt and 10.0×10^{-3} for the Fe^{III} salt at 295 K, about 10% larger compared with the corresponding TPP salts.[8,10]

Charge transport in $(PTMA)_x[M^{III}(Pc)(CN)_2]\cdot y(MeCN)$

The temperature dependence of the resistivity along the *b*-axis is shown in Fig. 3. The value at room temperature is 4.7×10^{-3} Ω cm for the Co^{III} salt and 1.6×10^{-2} Ω cm for the Fe^{III} salt. These fairly low resistivity values and metallic behavior at high temperature (>230 K for the Co^{III} salt and >270 K for the Fe^{III} salt) strongly support that they are partially oxidized salts. With lowering the temperature, the conduction shows thermally activated behavior. The difference of the resistivity between the Co^{III} and Fe^{III} salts becomes larger at low temperature. On the other hand, no difference in conductivity between the MeCN- and Me_2CO-inclusive crystals was observed.

Fig. 4 shows the temperature dependence of the thermoelectric power (Q). For both salts, the thermoelectric power shows clear metallic behavior at high temperatures. The values and the slope of the linear portion are relatively close to each other. The thermoelectric power of a metallic conductor with one-dimensional tight-binding band structure is given by eqn. (1),[18]

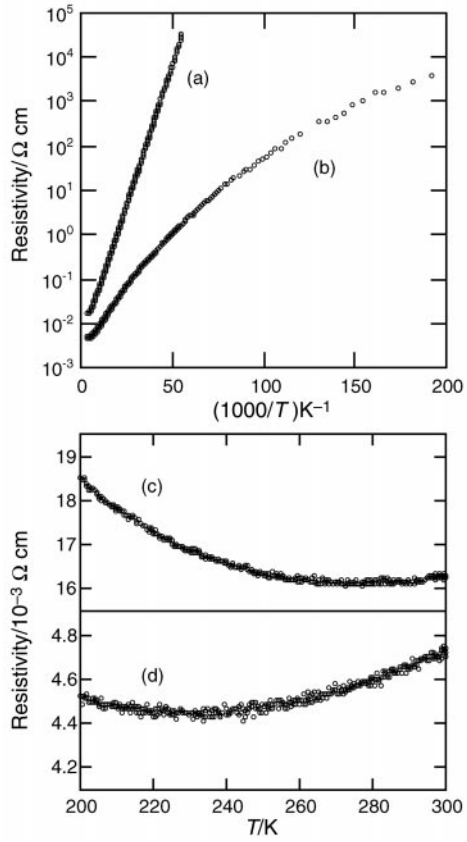

Fig. 3 Temperature dependence of the single-crystal resistivity (//*b*) of (a) $(PTMA)_x[Fe^{III}(Pc)(CN)_2]\cdot y(MeCN)$ and (b) $(PTMA)_x[Co^{III}(Pc)(CN)_2]\cdot y(MeCN)$, and corresponding curves in the high temperature region, (c) and (d).

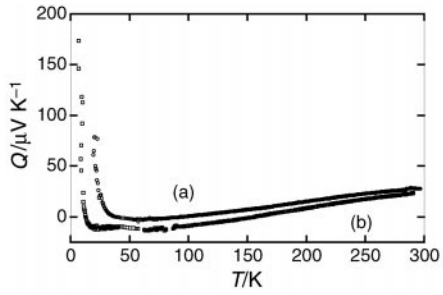

Fig. 4 Temperature dependence of the single-crystal thermoelectric power (*Q*, //*b*) of (a) $(PTMA)_x[Fe^{III}(Pc)(CN)_2]\cdot y(MeCN)$ and (b) $(PTMA)_x[Co^{III}(Pc)(CN)_2]\cdot y(MeCN)$.

$$Q = -\frac{\pi k_B^2 \cos\left(\frac{\pi v}{2}\right)}{6|e|t\sin^2\left(\frac{\pi v}{2}\right)}T \qquad (1)$$

where t is the transfer integral, k_B is the Boltzmann constant, e is the unit charge of an electron, and v is the number of conduction band electrons per site and equals $2-\rho$ for the oxidation number ρ. Since the overlap integrals in the PTMA salts are about 10% larger than those in the TPP salts, the band widths in the PTMA salts are estimated to be 0.51 eV for the Co^{III} salt and 0.57 eV for the Fe^{III} salt. By using one-quarter of each value as t in the equation, the oxidation number ρ can be calculated from the slope of *Q vs. T*. The value obtained is around 0.46 for both salts, indicating $\rho \approx 0.5$.

Compared with the resistivity data, the metallic region observed in the thermoelectric power measurements is much wider. The inconsistency between the thermoelectric power and conductivity might appear owing to the highly one-dimensional character and rather narrow band widths of the salts, as suggested for the TPP salts.[8,10]

A steep increase in the thermoelectric power appears at low temperature (<15 K for the Co^{III} salt and <35 K for the Fe^{III} salt). At these temperatures, no anomaly is observed in the resistivity data.

Magnetic susceptibility of $(PTMA)_x[M^{III}(Pc)(CN)_2]\cdot y(MeCN)$

The temperature dependence of the magnetic susceptibility of $(PTMA)_x[M^{III}(Pc)(CN)_2]\cdot y(MeCN)$ is shown in Fig. 5. The data are corrected for the background and the core diamagnetic contribution, and the stoichiometry is assumed as $x=0.5$ and $y=1$ as suggested by the thermoelectric power and structure analyses. For the Co^{III} salt, the small paramagnetic susceptibility is almost temperature-independent, suggesting the Pauli-like susceptibility. The value (2.85×10^{-4} emu mol^{-1}) is larger than that expected for a simple one-dimensional metal with a band width of 0.51 eV, indicating that the electron–electron correlation effect in this system is relatively large. It is however smaller than that of $TPP[Co^{III}(Pc)(CN)_2]_2$ (3.85×10^{-4} emu mol^{-1} for the $TPP_{0.5}[Co^{III}(Pc)(CN)_2]$ unit)[10] which is consistent with the larger band width in $(PTMA)_x[Co^{III}(Pc)(CN)_2]\cdot y(MeCN)$.

On the other hand, the paramagnetic susceptibility of $(PTMA)_x[Fe^{III}(Pc)(CN)_2]\cdot y(MeCN)$ shows a significant temperature dependence. In this salt, there are two kinds of spins: π-radical centered spin ($S=1/2$) and Fe^{III} centered spin ($S=1/2$). The concentration of the latter is twice that of the former. At high temperatures, the susceptibility nearly correlates to inverse temperature, suggesting Curie-like paramagnetism. At around 20 K, an anomaly that indicates the existence of antiferromagnetic interactions is apparent. The value and its temperature dependence resemble that of $TPP[Fe^{III}(Pc)(CN)_2]_2$.[10] In the TPP salt, highly anisotropic susceptibility was observed.[11] This feature made the analysis of the susceptibility of the randomly oriented sample difficult due to some possibility of preferential orientation. In the PTMA salt, a similar situation is expected. Since the crystal system of the PTMA salt is orthorhombic, the anisotropy measurement is more difficult compared with the tetragonal TPP salt.

As found in $TPP[Fe^{III}(Pc)(CN)_2]_2$,[11] giant negative magnetoresistance in $(PTMA)_x[Fe^{III}(Pc)(CN)_2]\cdot y(MeCN)$ has also

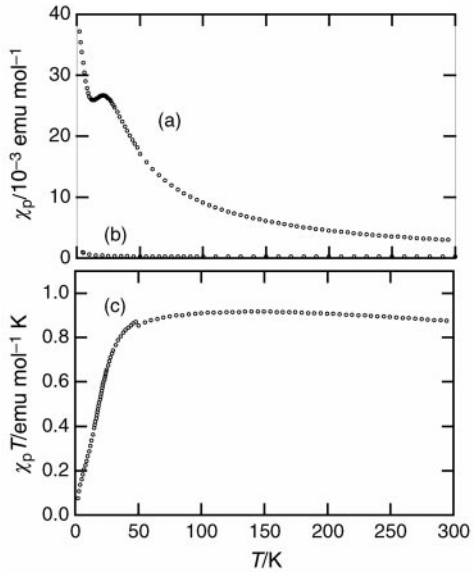

Fig. 5 Temperature dependence of the magnetic susceptibility (χ_p) of the randomly oriented polycrystalline samples; χ_p for (a) $(PTMA)_x[Fe^{III}(Pc)(CN)_2]\cdot y(MeCN)$ and (b) $(PTMA)_x[Co^{III}(Pc)(CN)_2]\cdot y(MeCN)$ and (c) χ_pT for $(PTMA)_x[Fe^{III}(Pc)(CN)_2]\cdot y(MeCN)$; $x=0.5$ and $y=1$.

been observed. The magnitude of the magnetoresistance observed in preliminary measurements is $R(8.8\ \mathrm{T})/R(0\ \mathrm{T}) = 0.44$ at 20 K [$R(H)$ is the resistance under a magnetic field H], which is comparable to that observed for TPP[Fe^{III}(Pc)$(CN)_2]_2$. This observation indicates the existence of π–d interactions in this system, since the alignment of the d-centered local magnetic moments by the external magnetic field causes a great influence on the motion of the π-centered charge carriers. Also, the appearance of antiferromagnetic interactions indicates the existence of the magnetic exchange interaction through the overlapped π-ligands, since the shortest $Fe^{III}\cdots Fe^{III}$ distance is more than 7 Å. Though the result is preliminary and further studies are required to elucidate the mechanism of the negative magnetoresistance, conductors based on the $Fe^{III}(Pc)(CN)_2$ unit are promising candidates as novel π–d systems.

In conclusion, we have found that the electrochemical oxidation of PTMA[M^{III}(Pc)$(CN)_2$] gives partially oxidized salts of (PTMA)$_x$[M^{III}(Pc)$(CN)_2$]·y(solvent) (M = Co or Fe and solvent = MeCN or Me_2CO) in which the solvent molecules partially occupy the cationic sites. They are highly conducting and metallic behavior is observed in the conductivity and thermoelectric power measurements. For the Fe^{III} salt, the existence of π–d interactions has been suggested from the magnetic and magnetoresistance measurements.

This work was partly supported by the Grant-In-Aid for Scientific Research, from the Ministry of Education, Science and Culture, Japanese Government and the Suhara Memorial Foundation.

References

1 C. S. Schramm, R. P. Scaringe, D. R. Stojakovic, B. M. Hoffman, J. A. Ibers and T. J. Marks, *J. Am. Chem. Soc.*, 1980, **102**, 6702; J. Martinsen, S. M. Palmer, J. Tanaka, R. Greene and B. M. Hoffman, *Phys. Rev. B*, 1984, **30**, 6269.
2 T. Inabe, T. J. Marks, R. L. Burton, J. W. Lyding, W. J. McCarthy, C. R. Kannewurf, G. M. Reisner and F. H. Herbstein, *Solid State Commun.*, 1985, **54**, 501.
3 T. Inabe, S. Nakamura, W. Liang, T. J. Marks, R. L. Burton, C. R. Kannewurf and K. Imaeda, *J. Am. Chem. Soc.*, 1985, **107**, 7224.
4 K. Yakushi, M. Sakuda, H. Kuroda, A. Kawamoto and J. Tanaka, *Chem. Lett.*, 1986, 1161.
5 T. Inabe and Y. Maruyama, *Bull. Chem. Soc. Jpn.*, 1990, **63**, 2273.
6 K. Morimoto and T. Inabe, *J. Mater. Chem.*, 1995, **5**, 1749.
7 A. Fujita, H. Hasegawa, T. Naito and T. Inabe, *J. Porphyrins Phthalocyanines*, 1999, **3**, 720.
8 H. Hasegawa, T. Naito, T. Inabe, T. Akutagawa and T. Nakamura, *J. Mater. Chem.*, 1998, **8**, 1567.
9 S. Takano, T. Naito and T. Inabe, *Chem. Lett.*, 1998, 1249.
10 M. Matsuda, T. Naito, T. Inabe, N. Hanasaki, H. Tajima, T. Otsuka, K. Awaga, B. Narymbetov and H. Kobayashi, *J. Mater. Chem.*, 2000, **10**, 631.
11 N. Hanasaki, H. Tajima, M. Matsuda, T. Naito and T. Inabe, *Phys. Rev. B*, 2000, **62**, 5839.
12 T. Inabe, *J. Porphyrins Phthalocyanines*, 2001, **5**, 3.
13 J. Metz and M. Hanack, *J. Am. Chem. Soc.*, 1983, **105**, 828.
14 A. Altomare, M. C. Burla, M. Camalli, M. Cascarano, C. Giacovazzo, A. Guagliardi and G. Polidori, *J. Appl. Crystallogr.*, 1994, **27**, 435.
15 teXsan: Crystal Structure Analysis Package, Molecular Structure Corporation, 3200 Research Forest Drive, The Woodlands, TX 77381, 1985 and 1992.
16 P. M. Chaikin and J. F. Kwak, *Rev. Sci. Instrum.*, 1975, **46**, 429.
17 Crystal data for PTMA[Fe^{III}(Pc)$(CN)_2$]: $C_{43}H_{30}N_{11}Fe_1$, $M = 756.63$, monoclinic, space group $P2_1/a$, $a = 8.703(1)$, $b = 21.870(4)$, $c = 18.401(3)$ Å, $\beta = 98.62(1)^\circ$, $U = 3462.7(9)$ Å^3, $Z = 4$, $D_c = 1.451$ g cm^{-3}, μ(Mo-Kα) = 0.487 mm^{-1}, $T = 113$ K. Full matrix least-squares refinement on F, anisotropic displacements for non-H atoms, 2544 independent reflections [$I > 3\sigma(I)$], 496 parameters, $R(F) = 0.077$, $R_w(F) = 0.088$.
18 P. M. Chaikin, J. K. Kwak, T. E. Jones, A. F. Garito and A. J. Heeger, *Phys. Rev. Lett.*, 1973, **31**, 601.